Available online at www.sciencedirect.com
ScienceDirect
Journal of Molecular Graphics and Modelling 25 (2006) 289–295
Journal of Molecular Graphics and Modelling
www.elsevier.com/locate/JMGM

Computational study of human phosphomannose isomerase: Insights from homology modeling and molecular dynamics simulation of enzyme bound substrate

Jingfa Xiao [a], Zongru Guo [a,*], Yanshen Guo [a], Fengming Chu [a], Piaoyang Sun [b]

[a] *Institute of Materia Medica, Chinese Academy of Medical Sciences and Peking Union Medical College, Beijing 100050, China*
[b] *Jiangsu Hengrui Medicine Co., Ltd., China*

Received 1 July 2005; received in revised form 4 January 2006; accepted 8 January 2006
Available online 20 February 2006

Abstract

Phosphomannose isomerase is a zinc metalloenzyme that catalyzes the reversible isomerization of mannose-6-phosphate and fructose-6-phosphate, and the three-dimensional (3D) structure of human phosphomannose isomerase has not been reported. In order to understand the catalytic mechanism, the 3D structure of the protein is built by using homology modeling based on the known crystal structure of mannose-6-phosphate isomerase from (PDB code 1PMI). The model structure is further refined by energy minimization and molecular dynamics methods. The mannose-6-phosphate–enzyme complex is developed by molecular docking and the key residues involved in the ligand binding are determined, which will facilitate the understanding of the action mode of the ligands and guide further genetic studies. Our results suggest a hydride transfer mechanism of α-hydrogen between the C1 and C2 positions but do not support the *cis*-enediol mechanism. The detailed mechanism involves, on one side, Zn^{2+} mediating the movement of a proton between O1 and O2, and, on the other side, the hydrophobic environment formed in part by Tyr^{278} promoting transfer of a hydride ion.

Keywords: Mannose-6-phosphate (M6P); Phosphomannose isomerase (PMI); Homology modeling; Molecular dynamics simulation

1. Introduction

Phosphomannose isomerase (PMI, EC 5.3.1.8) is a zinc metalloenzyme that catalyzes the reversible isomerization of mannose-6-phosphate (M6P) and fructose-6-phosphate (F6P; Fig. 1). This reaction is the first committed step in the synthesis of mannosylated glycoproteins from glycolytic intermediates and the enzyme plays an essential role in yeast cell wall biosynthesis [1,2]. In all eukaryotes and prokaryotes investigated so far, the enzyme has been reported to play a crucial role in both D-mannose metabolism and the supply of the activated mannose donor guanosine diphosphate D-mannose (GDP-D-mannose), which is a required reactant for the biosynthesis of many mannosylated structures, including glycoproteins, glycolipids, and, cell wall components. PMIs are considered to be potential therapeutic targets because of their role in survival and pathogenesis in several microbes such as *Saccharomyces cerevisiae* [2], *Candida albicans* [3], *Mycobacterium smegmatis* [4] and *Leishmania mexicana* [5]. In humans, a deficiency of PMI activity leads to carbohydrate-deficient glycoprotein syndrome type 1b (CGDS 1b), a severe metabolic disorder with hepatic-intestinal symptoms [6,7]. Today, this disease is successfully treated by oral D-mannose [8]. Due to the high level of amino acid sequence identity (>40%) between the pathogenic microorganisms type I PMIs and humans type I PMIs, especially for the binding site region, it appears that it might be difficult to achieve species-specific inhibition of a fungal or bacterial type I PMI but not have the inhibition for humans type I PMI. On the other hand, no sequence identity is found between type I and type II enzymes, except for a very small conserved amino acid sequence motif, which makes up part of the active site in the crystal structure [9]. Therefore, specific inhibition of the PMI activity, while leaving the human type I protein unaffected, should be achieved more easily for type II than for type I pathogenic proteins [10]. This suggests the possibility of rational design of potent and highly species-specific inhibitors against the targeted PMIs from pathogens.

* Corresponding author. Tel.: +86 1063165249; fax: +86 1083155752.
E-mail address: zrguo@imm.ac.cn (Z. Guo).

1093-3263/$ – see front matter
doi:10.1016/j.jmgm.2006.01.001

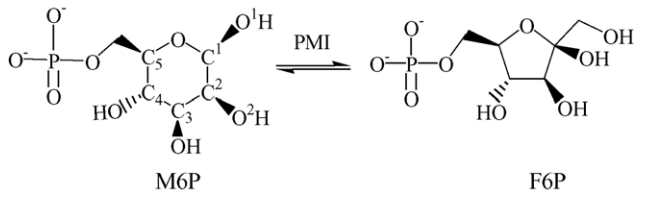

Fig. 1. A scheme of reversible interconversion of M6P and F6P catalyzed by phosphomannose isomerases.

The type I PMI isolated from *S. cerevisiae* [11] in 1968 has been shown to be a zinc-dependent metalloenzyme [12]. An X-ray crystal structure of the type I PMI from *C. albicans* has been reported [13]. In this report, the active site and a zinc metal cofactor binding site were identified; however, the roles of the individual active site amino acids and the catalytic mechanism are still not known. A reaction mechanism was proposed in which the zinc coordinates with the carbonyl and hydroxyl oxygens on Cl and C2, thereby activating the hydrogen α to the carbonyl, which is abstracted by the nonprotonated nitrogen of an imidazole group to form the transient enediol intermediate [12].

The elucidation of the catalytic mechanisms of type I and type II PMIs is strongly needed for rational drug design since the PMIs have been considered as potential therapeutic targets. Up until now, inhibition and crystallographic details of all PMIs are still largely unexplored. Hence, as part of our program of study on aldose–ketose isomerases, we have initiated homology studies with the objective of revealing the molecular architecture of the active site as the structural framework for catalysis. The 3D features of the model are obtained by a homology modeling procedure based on the crystal structure of mannose-6-phosphate isomerase from *C. albicans* (PDB code 1PMI) [13]. Homology modeling is an efficient method for the 3D structure construction of a protein [14]. In order to explain substrate specificity and the structure–function relationship of the enzyme, a docking simulation of the phosphomannose isomerase–M6P complex was performed by the Affinity module in InsightII. The information on the M6P binding domain of these enzymes is important to understand the catalytic mechanism of PMI and can further help us to design selective inhibitors.

2. Theory and methods

All calculations were performed on the SGI Fuel workstations using the InsightII software package developed by Biosym Technologies [15]. The amino acid sequences of human phosphomannose isomerase (entry NF00118844) were retrieved from the PIR protein sequence database. In the energy minimization and molecular dynamics calculations, the consistent force field (CFF) [16,17] was employed. The secondary structures were assigned by using the DSSP program [18].

2.1. 3D model building

The homology module [19] was used to build the initial model of human phosphomannose isomerase. The homologous protein was searched by the Fasta program. The first requirement in the construction of the human phosphomannose isomerase (*h*PMI) model structure is a multiple sequence alignment among these templates. The sequence alignment is based on identifying structurally conserved regions (SCRs) common to the three templates. Three reference proteins are mannose-6-phosphate isomerase from *C. albicans* (1PMI) [13], mannose-6-phosphate isomerase from *Bacillus subtilis* (1QWR), and glucose-6-phosphate isomerase from Human (1JLH) [20]. The next step is to generate a multiple sequence alignment of human phosphomannose isomerase with the three templates. This step is also based on the identification of SCRs common to template and target [21]. The sequence identity between human phosphomannose isomerase and reference protein mannose-6-phosphate isomerase from *C. albicans* (PDB code 1PMI) [13] is 40.9% (*Ca*PMI). An initial 3D structure of *h*PMI was obtained by transferring the backbone coordinates of the mannose-6-phosphate isomerase from *C. albicans* residues to the corresponding residues of *h*PMI, except for several variable regions (LOOPs). To construct the structural variable regions, a loop-searching and generating algorithm [22] over the databank of known crystal structures was used. The residues at the N-terminus and C-terminus were generated through end-repair by using the InsightII/Homology program. The divalent metal ion Zn^{2+} coordinates of *h*PMI were obtained by transferring the Zn^{2+} coordinates of *Ca*PMI. Through the procedure mentioned above, an initial 3D model was thus completed.

The refinement of the homology model was carried out through energy minimization: 500 iterations of steepest descent (SD) calculation were performed and then the conjugated gradient (CG) calculation was carried out until achieving 0.1 kcal/mol $Å^{-1}$ of convergence on the gradient. After simulations, the homology model was obtained by means of the molecular dynamics (MD) calculation with the use of the Discover 3 software package [23]. All simulations were carried out using the NVT ensemble at a temperature of 298 K. The homology model was solvated with a 15 Å CFF model water cap from the center of mass of *h*PMI. Aspartate, glutamate, arginine and lysine residues are charged and all the tyrosine residues are neutral. The SHAKE algorithm [24] was used to constrain the bonds containing hydrogens to their equilibrium length. The Verlet leapfrog algorithm was used to integrate the equations of motion [25]. Finally, a conjugate gradient energy minimization of the full protein was performed until the root mean-square (rms) gradient energy was lower than 0.01 kcal/mol $Å^{-1}$. In this step, the quality of the initial model is improved. After the optimization procedure, the structure was checked by Profile-3D [26,27] and ProStat. Profile-3D tests the validity of the hypothetical protein structures, by measuring the compatibility of the hypothetical structure with its own amino acid sequence. This is especially useful in the final phase of protein structural modeling. The ProStat module of InsightII identifies and lists the number of instances where structural features differ significantly from the average values calculated from known proteins.

2.2. Docking substrate into the active site

Molecular docking can fit molecules together with a favorable configuration to form a complex system. The structural information from the theoretical modeled complex can help us to understand the catalytic mechanism of an enzyme. The sugar of M6P contains two structural forms namely linear form and cyclic form. In order to determining what form of sugar binds preferentially to the enzyme, both the linear and cyclic forms of the sugar are docked. Structures of the linear form and cyclic form of M6P were built using the Builder Molecule function and minimized with CFF, with an energy convergence cut-off of 0.001 kcal/mol. The phosphate groups of mannose-6-phosphate were treated as the ionization state. To track the interacting mode of *h*PMI with M6P, the advanced docking program Affinity [28] is used to fulfil the automated molecular docking. The best binding structure of the ligand to the receptor based on the energy of the ligand/receptor complex was automatically found by Affinity, which uses a combination of Monte Carlo type and Simulated Annealing procedures to dock a guest molecule to a host one. The potential function of the complex is assigned by using the CFF and the atom-based approach [29] is used for nonbonded interactions. To account for the solvent effect, the centered enzyme–substrate complexes are solvated in a sphere of water molecules with a radius of 15 Å. Any solvent molecule within 2.8 Å of a heavy atom of the enzyme is deleted. Finally, the docked complexes of *h*PMI and mannose-6-phosphate are selected according to the criteria of interaction energy combined with geometrical matching quality. These complexes are used as the starting conformation for further energetic minimization and molecular dynamics simulations before the final models are achieved.

3. Results and discussions

3.1. Homology modeling of hPMI

An optimal sequence alignment is essential to the success of homology modeling. Three reference proteins, mannose-6-phosphate isomerase from *C. albicans* (1PMI) [13], mannose-6-phosphate isomerase from *B. subtilis* (1QWR), and glucose-6-phosphate isomerase from Human (1JLH) [20], were used to model the structure of human mannose-6-phosphate isomerase. The homology scores for the three reference proteins compared with *h*PMI were 40.9%, 23.2%, and 21.0%, respectively. Phosphomannose isomerase is a zinc metalloenzyme that is involved in the reversible isomerization of mannose-6-phosphate and fructose-6-phosphate. The series of phosphomannose isomerase from different organism exhibits extensive sequence similarity and shares a common mechanism. In order to define structural conservative regions (SCRs) of the protein family, multi-dimensional alignment was used to superimpose the three reference structures, and the nine SCRs were determined. The Needleman–Wunsch algorithm with the identity matrix was used to align the amino acid sequence of *h*PMI to the SCRs. For comparison, we chose the closest

Fig. 2. Sequence alignment of human mannose-6-phosphate isomerase with template protein mannose-6-phosphate isomerase from *Candida albicans* (PDB code 1PMI); the α-helices are represented by green color and β-sheets are represented by yellow color.

reference protein *Ca*PMI [13] as the template protein for modeling *h*PMI (see Fig. 2). The LOOPs between SCRs are more variable in conformation among the different reference proteins. The loop-searching and generating algorithm was used to construct the structure of LOOPs. The sidechain conformations were selected to add to the protein backbone based on a backbone-dependent rotamer library and the optimum conformation is defined as that with the lowest nonbonded energy. The structural optimization is proceeded with using energy minimization and molecular dynamics methods and the final structure of *h*PMI. The secondary structure was calculated using the DSSP program and is presented in Fig. 3. From Fig. 3 it can be seen that the enzyme contains 18 β-strands and 11 α-helices and consists of two

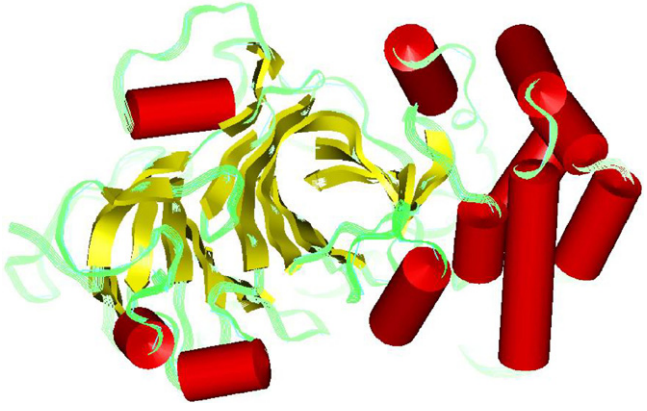

Fig. 3. The final 3D structure of human mannose-6-phosphate isomerase. The α-helix is represented by red color and the β-sheet is represented by green color.

mixed five-stranded β-sheets surrounded by α-helices. The two sheets that form the cupin domain have seven and five strands, respectively, and between them a deep pocket with approximate dimensions 5 Å × 8 Å × 8 Å can be observed (Fig. 3). The cupin domain is similar to that described for phosphoglucose isomerase from *Pyrococcus furiosus* [30] and mannose-6-phosphate isomerase from *C. albicans* [13]. The quality of the homology model was further evaluated by Profile-3D and ProStat. For the *h*PMI model, the stereochemical quality is checked by ProStat and there is not the case appeared that the bond lengths and bond angles are different significantly from the average values calculated from known proteins in the total residues. The compatibility between the amino acid sequence and the environment of the amino acid sidechains in the model is another validation criterion. Here its compatibility scores are obtained by using Profile-3D and the corresponding results for the *h*PMI model and template protein *Ca*PMI are shown in Fig. 4. It should be noted that compatibility scores above zero correspond to 'acceptable' sidechain environment. From Fig. 4, it can be seen that the positions of all residues are reasonable except the residue Ser^{33}. Fortunately, the residue Ser^{33} located far from the active site of the enzyme. So the poor building of this residue should have not much influence on the subsequent study. All of these data make us to believe that the model structure of *h*PMI is reliable.

Analysis of the sequence conservation between these PMIs and the putative PMIs identified by alignment of genome sequence data from Chimpanzee, *Vibrio cholerae*, *L. mexicana*, House mouse, *Homo*, *Filobasidiella neoformans*, *Emericella nidulans*, and *C. albicans* reveals striking conservation at one end of the pocket formed between the two β-sheets of the cupin domain and involving the four metal-binding ligands Gln^{111}, His^{113}, Glu^{138}, and His^{285} (using the *C. albicans* numbering). For the *h*PMI the four metal-binding residues are Gln^{110}, His^{112}, Glu^{137}, and His^{276}, and corresponding distances involved in his interaction are Gln^{110} (2.59 Å), His^{112} (2.79 Å), Glu^{137} (2.11 Å),

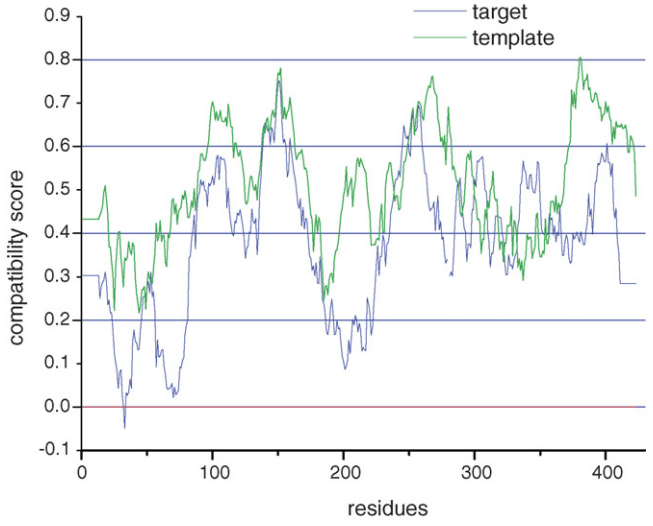

Fig. 4. The verification by profile 3D of our results for human mannose-6-phosphate isomerase and template protein; residues with positive compatibility score are reasonably folded.

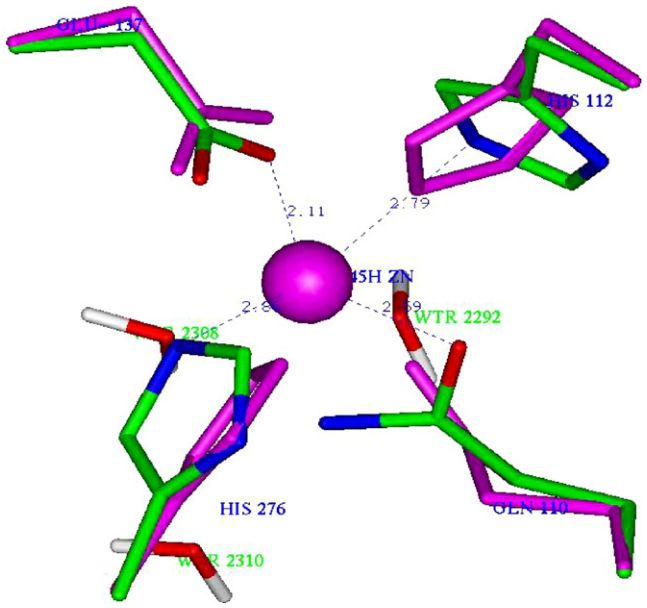

Fig. 5. The comparison of interaction mode of Zn^{2+} with *h*PMI and *Ca*PMI. The binding site residues of *Ca*PMI are represented by purple color, the metal ion is shown in ball mode and the residues involved in the interaction with enzyme are represented by stick form.

and His^{276} (2.86 Å) (Fig. 5). Comparison of the X-ray crystallographic structures of 12 zinc-containing enzymes [31] led to the conclusion that zinc-binding sites in enzymes favor histidine as the principal ligand. In *P. furiosus* phosphoglucose isomerase the four residues that form the metal-binding ligands (His^{88}, His^{90}, Glu^{97}, and His^{136}) differ only in the replacement of one of the glutamine by a histidine [30]. Also seen was the significant conservation of the hydrophobic residues $Tyr^{278}$and Leu^{270}, and polar residues Lys^{135} and Glu^{285}, which are located in this pocket. In addition, the zinc also coordinated with the three water molecules WTR^{2310}, WTR^{2308} and WTR^{2292}.

3.2. Interaction between hPMI and M6P

In order to understand the interaction between *h*PMI and M6P, the complex of *h*PMI and M6P was developed by the Affinity module. The probable 3D binding conformations and hydrogen bonding interactions of the complex of *h*PMI with cyclic form and linear form of M6P are shown in Figs. 6 and 7, respectively.

For the complex of *h*PMI and the cyclic form of M6P, the contact between the enzyme and substrate are shown in Fig. 6. In one of the orientations the phosphate group is bound by an arginine–lysine cluster (Arg^{295}, and Lys^{301}). The sugar phosphate is held by the salt bridge interaction and potential hydrogen bonds with Arg^{295}. The hydroxyl at C3 forms a hydrogen bond with the hydroxyl O of Ser^{108}, as does hydroxyl at C4 with amide nitrogen of Arg^{295} (in Table 1). The hydroxyl at C2 of M6P does not directly contact with the protein but is involved in hydrogen bonding with Tyr^{278} via the bridge of water molecule WTR^{2310}. The above-mentioned interactions would place the C1 and C2 of M6P deep in the pocket, adjacent to the transition metal center and nearby the side chains of

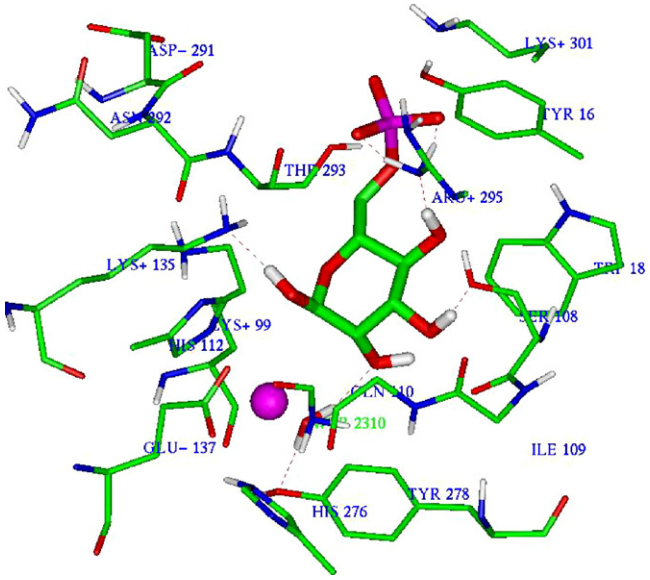

Fig. 6. The binding mode of the cyclic form of M6P bound to the active site region of *h*PMI. The M6P and residues are represented by stick mode, and the Zn^{2+} is represented by ball mode.

Lys[135] and His[112] and the more remote side chain of Glu[137] (Fig. 6). The hydroxyl at C1 forms hydrogen bonding with the side chain amide nitrogen of Lys[135]. The O at ring is within hydrogen bonding distance of the side chain amide nitrogen of Lys[135], which donates a proton to the ring oxygen. This Lys[135] residue may be one of the amino acids that catalyze ring opening of M6P in the enzyme *h*PMI. For the complex of *h*PMI and the linear form of M6P, the contact between the enzyme and substrate are shown in Fig. 7. The sugar phosphate group is held by the salt bridge interaction and potential hydrogen bonds with Arg[295], which anchor the C1 and C2 of M6P deep in the pocket, adjacent to the transition metal center. The zinc contacts the C2 hydroxyl and C1 carbonyl with the distances of 2.09 and

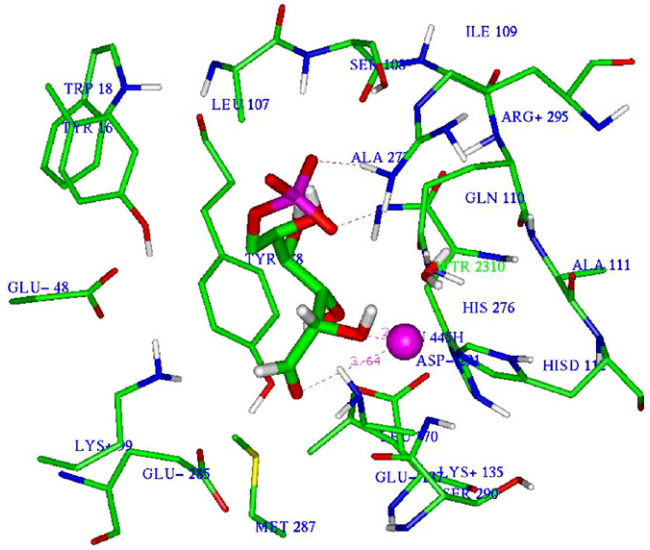

Fig. 7. The binding mode of the linear form of M6P bound to the active site region of *h*PMI. The M6P and residues are represented by stick mode, and the Zn^{2+} is represented by ball mode.

Table 1
The hydrogen bonds between the cyclic form of M6P and the binding pocket residues of human phosphomannose isomerase

Human phosphomannose isomerase		M6P (atom)	Distance (Å)	Angle (°)
Residue	Atom			
Arg^{295}	NH	Phosphate O	1.49	147.9
Arg^{295}	NH	Phosphate O	1.48	153.7
Lys^{135}	N	Mannose OH	1.88	176.5
Ser^{108}	O	Mannose OH	1.73	165.0
Arg^{295}	N	Mannose OH	1.52	161.7

2.64 Å, respectively. In the binding of M6P both O1 and O2 become coordinated to the Zn^{2+} by displacing the two water molecules, WTR^{2292} and WTR^{2308} from the coordination shell, leaving only a water molecule of WTR^{2310} to interact with the Zn^{2+}. Compared to the complex of *h*PMI and the cyclic form of M6P, the interaction of Zn^{2+} and M6P is enhanced. The C1 and C2 of M6P are also located within the hydrophobic environment formed by Tyr^{278} and Met^{287}.

3.3. Catalytic mechanism

The reaction catalyzed by PMI is an aldose–ketose isomerization in which a hydrogen atom is transferred between the C1 and C2 positions of the substrate. A second hydrogen, in the form of a proton, also moves between the O1 and O2. The carbon-bound hydrogen can move by one of two mechanisms (in Fig. 8), a hydride shift or a proton transfer via a *cis*-enediol intermediate [32]. In isomerases that contain a metal ion at the catalytic center the mechanism appears to be a hydride shift, e.g. xylose isomerase [33], whereas isomerases without a metal cofactor use the *cis*-enediol mechanism [32]. Which mechanism operates in *h*PMI? A reaction mechanism was proposed by

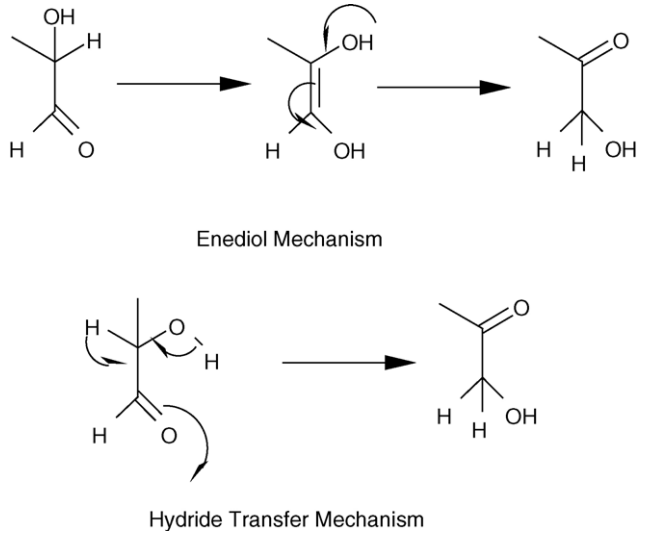

Fig. 8. Alternative mechanisms for hydrogen transfer in aldose–ketose isomerase (after Ref. [32]). The hydrogen can move either as a solvent-exchangeable proton in a *cis*-enediol mechanisms (top) or directly as a non-exchangeable hydride (bottom).

Gracy and Noltmann [12] in which the zinc coordinates with the carbonyl on C1 and hydroxyl oxygens on C2, thereby activating the α-hydrogen to the carbonyl, which is abstracted by the nonprotonated nitrogen of an imidazole group to form the transient enediol intermediate. While the catalytic base in that model [12] was one of the imidazole groups in the active site from pK_a measurements, the structural study on PMI from *C. albicans* was not conclusive as to which amino acids are essential to the reaction [13]. In order to understand the interaction between enzyme and substrates clearly and discuss the catalytic mechanism, the schematic summaries of the interaction of *h*PMI with cyclic form of M6P and linear form of M6P are listed in Fig. 9a and b, respectively. From the docking

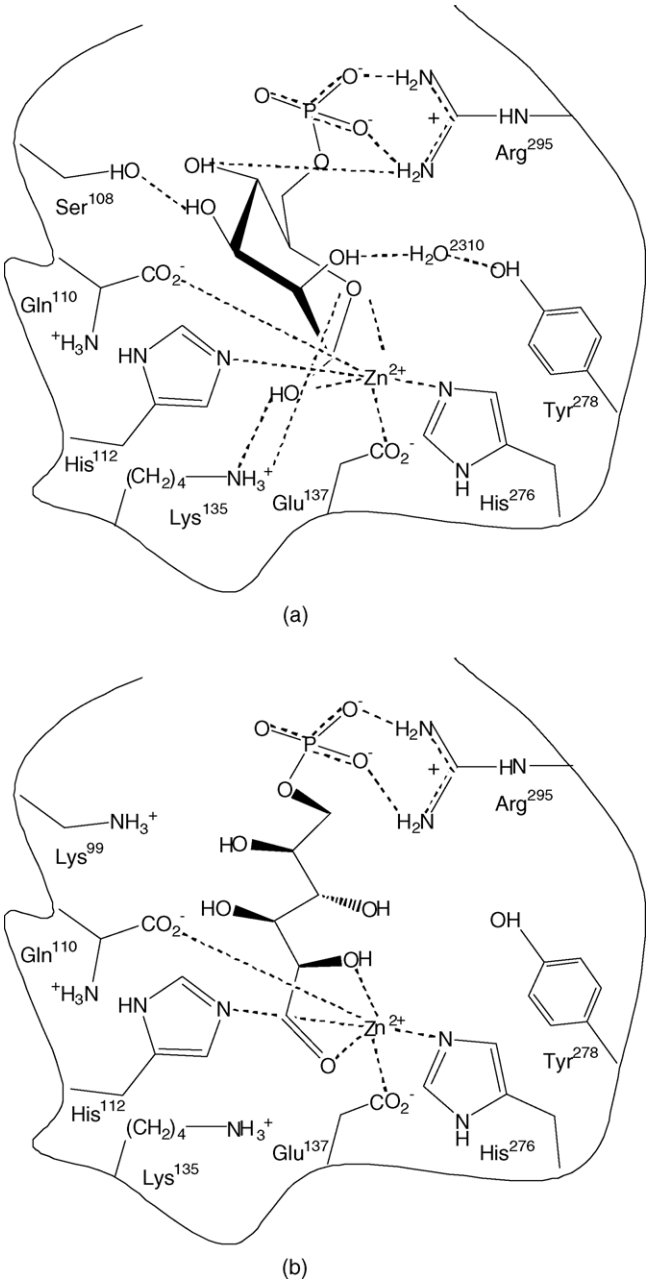

Fig. 9. Schematic summary of the interaction of *h*PMI with cyclic form of M6P (a) and linear form of M6P (b). Residues relevant to this study (Lys^{99}, Ser^{108}, Gln^{110}, His^{112}, Lys^{135}, Glu^{137}, His^{276}, Tyr^{278} and Arg^{295}) are shown.

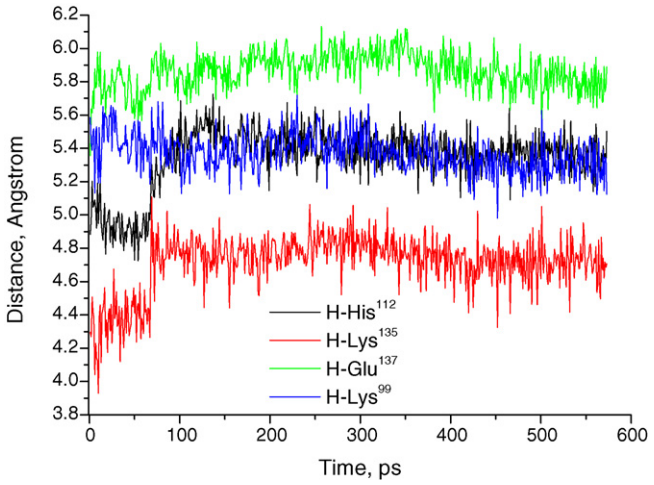

Fig. 10. Distances of C2 α-hydrogen of M6P to N of His^{112} (represented by black color), amide nitrogen of Lys135 (represented by red color), carboxyl O of Glu^{137} (represented by green color) and amide nitrogen of Lys99 (represented by blue color).

results, we can see that the enzyme binds preferentially to the cyclic forms. But, the process of ring opening is required prior to isomerization from M6P to fructose-6-phosphate. The Lys^{135} residue may be one of the amino acids that catalyze ring opening of M6P in the enzyme *h*PMI (Fig. 9a). In the complex of *h*PMI and linear form of M6P (Fig. 9b), the zinc coordinates with the carbonyl on C1 and hydroxyl on C2, which can mediate the movement of a proton between O1 and O2. In the vicinity of Cl and C2 there are five residues Lys^{135}, His^{112}, Lys^{99}, Met^{287} and Glu^{137}. Only the four residues of Lys^{135}, His^{112}, Lys^{99}, and Glu^{137}may act as the basic catalytic amino acid for the C2 α-hydrogen. To gain insight into the mechanism of the α-hydrogen transfer, we modeled the complex of *h*PMI-M6P by molecular dynamics simulation. At any time during the MD simulation, the average distance between the C2 α-hydrogen of M6P and the functional group of Lys^{135}-NH_2, His^{112}-N, Lys^{99}-NH_2 and Glu^{137}-CO_2^- were 4.75, 5.40, 5.35 and 5.82 Å (Fig. 10), respectively. From the MD simulation we can see that, there are no suitable residues in the region of the active site that could deprotonate the C2, and an enediol mechanism for *h*PMI is therefore considered unlikely. Given this, we favor a hydride transfer mechanism for *h*PMI as shown in Fig. 8 in the M6P to F6P direction. On one side, Zn^{2+} mediates the movement of a proton between O1 and O2, and, on the other side, the hydrophobic environment formed in part by Tyr^{278} promotes transfer of a hydride ion. But, the main role of these conservative residues Gln^{110}, His^{112}, Glu^{137}, and His^{276} is only to locate the Zn^{2+} and balance the charge on the metal ion in the catalytic process. The same mechanism of the phosphoglucose isomerase from *P. furiosus* was proposed by the Swan group [34].

4. Conclusions

The 3D structure of the protein was built by using homology modeling based on the known crystal structure of mannose-6-phosphate isomerase from *C. albicans* (PDB code 1PMI).

The model structure was further refined by energy minimization and molecular dynamics methods. The enzyme is a typical metalloenzyme that has a cupin domain. The carbon-bound hydrogen can move by one of two possible mechanisms, a hydride shift or a proton transfer via a *cis*-enediol intermediate. Our results support the hydride transfer mechanism of the α-hydrogen between the C1 and C2 positions and not the *cis*-enediol mechanism. The detailed mechanism shows that, on one side, Zn^{2+} mediates the movement of a proton between O1 and O2, and, on the other side, the hydrophobic environment formed in part by Tyr^{278} promotes transfer of a hydride ion. The binding site residue, Arg^{295}, plays an important role in the substrate binding via salt bridge interaction with the phosphate group of M6P.

References

[1] P. Orlean, Mol. Cell. Biol. 10 (1990) 5796–5805.
[2] M.A. Payton, M. Rheinnecker, L.S. Klig, M. DeTiani, E. Bowden, J. Bacteriol. 173 (1991) 2006–2010.
[3] D.J. Smith, A.E.I. Proudfoot, M. De Tiani, T.N.C. Wells, M.A. Payton, Yeast 11 (1995) 301–310.
[4] J.H. Patterson, R.F. Waller, D. Jeevarajah, H. Billman-Jacobe, M. McConville, Biochem. J. 372 (2003) 77–86.
[5] A. Garami, T. Ilg, J. Biol. Chem. 276 (2001) 6566–6575.
[6] T.J. De Koning, L. Dorland, O.P. Van Diggelen, A.M.C. Boonman, G.J. De Jong, W.L. Van Noort, J. De Schryver, M. Duran, I.E.T. Van den Berg, G.J. Gerwig, R. Berger, B.T. Poll-The, Biochem. Biophys. Res. Commun. 245 (1998) 38–42.
[7] J. Jaeken, G. Matthijs, J.M. Saudubray, C. Dionisi-Vici, E. Bertini, P. De Lonlay, H. Henri, H. Carchon, E. Schollen, E. Van Schaftingen, Am. J. Hum. Genet. 62 (1998) 1535–1539.
[8] C.J. Hendriksz, P. McClean, M.J. Henderson, D.G. Keir, V.C. Worthington, F. Imtiaz, E. Schollen, G. Matthijs, B.G. Winchester, Arch. Dis. Child. 85 (2001) 339–340.
[9] S.O. Jensen, P.R. Reeves, Biochim. Biophys. Acta 1382 (1998) 5–7.
[10] B. Wu, Y. Zhang, R. Zheng, C. Guo, P.G. Wang, FEBS Lett. 519 (2002) 87–92.
[11] R.W. Gracy, E.A. Noltman, J. Biol. Chem. 243 (1968) 3161–3168.
[12] R.W. Gracy, E.A. Noltman, J. Biol. Chem. 243 (1968) 4109–4116.
[13] A. Cleasby, A. Wonacott, T. Skarzynski, R.E. Hubbard, G.J. Davies, A.E.I. Proudfoot, A.R. Bernard, M.A. Payton, T.N.C. Wells, Nat. Struct. Biol. 3 (1996) 470–479.
[14] F. Eisenhaber, B. Persson, P. Argos, Crit. Rev. Biochem. Mol. Biol. 30 (1995) 1.
[15] InsightII, Version 98.0, MSI, San Diego, 1998.
[16] J.R. Maple, M.J. Hwang, T.P. Stockfisch, U. Dinur, M. Waldman, C.S. Ewig, A.T. Hagler, J. Comp. Chem. 15 (1994) 162–182.
[17] M.J. Hwang, T.P. Stockfisch, A.T. Hagler, J. Am. Chem. Soc. 116 (1994) 2515–2525.
[18] W. Kabsch, C. Sander, Biopolymers 22 (1983) 2577–2637.
[19] Homology User Guide, MSI, San Diego, USA, 1999.
[20] A.T. Cordeiro, P.H. Godoi, C.H. Silva, R.C. Garratt, G. Oliva, O.H. Thiemann, Biochem. Biophys. Acta 1645 (2003) 117–122.
[21] S.B. Needleman, C.D. Wunsch, J. Mol. Biol. 48 (1970) 443–453.
[22] P.S. Shenkin, D.L. Yarmush, R.M. Fine, H. Wang, C. Levinthal, Biopolymers 26 (1987) 2053–2085.
[23] Discover 3 User Guide, MSI, San Diego, USA, 1999.
[24] J.P. Ryckaert, G. Ciccotti, H.J.C. Berendsen, J. Comput. Phys. 23 (1977) 327–341.
[25] L. Verlet, Phys. Rev. 159 (1967) 98–103.
[26] Profile-3D User Guide, MSI, San Diego, USA, 1999.
[27] R. Luthy, J.U. Bowie, D. Eisenberg, Nature 356 (1992) 83–85.
[28] Affinity User Guide, MSI, San Diego, USA, 1999.
[29] H.Q. Ding, N. Karasawa, W.A. Goddard III, J. Chem. Phys. 97 (1992) 4309.
[30] J.M. Berrisford, J. Akerboom, A.P. Turnbull, D. DeGeus, S.E. Sedelnikova, I. Staton, C.W. McLeod, C.H. Verhees, J. van der Oost, D.W. Rice, P.J. Baker, J. Biol. Chem. 278 (2003) 33290–33297.
[31] B.L. Valee, D.S. Auld, Biochemistry 29 (1990) 5647–5659.
[32] I.A. Rose, Adv. Enzymol. Relat. Areas Mol. Biol. 43 (1975) 491–517.
[33] M. Whitlow, A.J. Howard, B.C. Finzel, T.L. Poulos, E. Winbourne, G.L. Gilliland, Proteins 9 (1991) 153–173.
[34] M.K. Swan, J.T. Solomons, C.C. Beeson, T. Hansen, P. Schonheit, C. Davies, J. Biol. Chem. 278 (2003) 47261–47268.